Available at www.sciencedirect.com

INFORMATION PROCESSING IN AGRICULTURE xxx (xxxx) xxx

journal homepage: www.keaipublishing.com/en/journals/information-processing-in-agriculture/

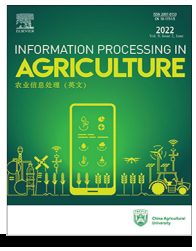

Evaluation of UAV spraying quality based on 1D-CNN model and wireless multi-sensors system

Ziyuan Hao, Minzan Li, Wei Yang *, *Xinze Li*

Key Laboratory of Smart Agriculture Systems, Ministry of Education, China Agricultural University, Beijing 100083, PR China

ARTICLE INFO

Article history:
Received 15 January 2022
Received in revised form
14 June 2022
Accepted 31 July 2022
Available online xxxx

Keywords:
UAV
Spraying quality
Droplet deposition
1D-CNN model
Sensor

ABSTRACT

The droplet deposition is a key index to evaluate the quality of unmanned aerial vehicle (UAV) spraying. The detection of the droplet deposition is time-consuming and costly, therefore, it is difficult to achieve large-scale and rapid acquisition in the field. To solve the above problems, a droplet deposition acquisition system (DDAS) was developed. It was composed of the multiple sensors, processing units, remote server database and Android-based software. A droplet deposition prediction model based on field experimental data was established by using a one-dimensional convolutional neural network (1D-CNN) algorithm, and the effects of different inputs on the prediction ability of the model were analyzed. The results showed that adding temperature and humidity data to the inputs can achieve higher prediction accuracy than only using UAV spraying operation parameters and wind speed data as the inputs to the model. In addition, the prediction accuracy of the 1D-CNN model was the highest when compared with other models such as back propagation neural network, multiple correlation vector machine, and multiple linear regression. The 1D-CNN model was embedded into the DDAS, and the evaluation experiments were carried out in the field. The correlation analysis was conducted between two datasets of the droplet deposition obtained by the DDAS and water sensitive paper (WSP), respectively. The R^2 was 0.924, and the RMSE was 0.026 μL/cm^2. It is proved that the droplet deposition values obtained by the DDAS and WSP have high consistency, and the DDAS developed can provide an auxiliary solution for the intelligent evaluation of UAV spraying quality.

1. Introduction

Unmanned aerial vehicle (UAV) has been widely applied in agriculture [1], such as spraying pesticides in fields to control pests and crop diseases [2]. UAV has a higher spraying height and a smaller droplet size than the traditional artificial backpack sprayer and self-propelled ground-spraying equipment. However, the droplets are difficult to reach the target crop in some cases because the droplet deposition of UAV drifts easily [3]. Therefore, the quality of UAV spraying should be tested and evaluated to determine the optimal spraying parameters for the droplet deposition to reach the target crop. Droplet deposition is an important index and represents the volume of droplets deposited per unit area. Accurate droplet deposition can help in making reasonable spraying decisions, improving spraying quality, and reducing pesticide consumption [4].

Obtaining the droplet deposition is complicated, and the related researches have been conducted. The methods of

* Corresponding author.
E-mail address: cauyw@cau.edu.cn (W. Yang).

Peer review under responsibility of China Agricultural University.
https://doi.org/10.1016/j.inpa.2022.07.004

Please cite this article as: Z. Hao, M. Li, W. Yang et al., Evaluation of UAV spraying quality based on 1D-CNN model and wireless multi-sensors system, Information Processing in Agriculture, https://doi.org/10.1016/j.inpa.2022.07.004

obtaining the droplet deposition are mainly of two types, collecting droplets to detect the droplet deposition and building models to predict droplet deposition. Water sensitive paper (WSP) is usually used for collecting droplets after UAV spraying, and then the image processing method is adopted to analyze droplet deposition information [5]. This method allows the direct observation of the deposition effect. However, the accuracy of droplet deposition detection is influenced by the overlap of droplets on the WSP and limited by the scanner resolution [6]. In some studies, droplet deposition is indirectly obtained by calculating and analyzing the amount of tracer added to pesticides [7]. The tracer method can sensitively detect the deposition of droplets with low-cost raw materials. However, subsequent processing and complex analysis are needed to obtain the droplet deposition. Several commercial products for detecting the droplet deposition, such as laser particle size analyzers [8] and leaf wetness sensors [9], are also available. In addition, analytical balance is also necessary to directly measure the amount of droplet deposition [10]. This type of facility is accurate in terms of measuring the amount of droplet deposition. However, this facility is very expensive, mostly used in academic research, and unsuitable for agricultural production. Consequently, the low-cost and real-time detection of droplet deposition after spraying remains a challenge.

The droplet deposition of UAV spraying is influenced by many factors, such as the spraying parameters (spraying rates, spraying times, droplet sizes, and sprinkler speed), the UAV flight states (flight height and flight speed), environmental factors (humidity, temperature, and wind speed), and the liquid properties (liquid type and concentration) [11–13]. Several prediction models for droplet deposition based on different conditions have been studied. The computational fluid dynamics (CFD) model is a common method for predicting droplet deposition [14]. This model can effectively simulate various parameter states during spraying with high prediction accuracy. However, this method is mostly used in simulation and cannot easily achieve real-time prediction with field related sensors. Several researchers have adopted regression analysis methods to build the prediction model of droplet deposition, which can be conveniently applied to real-time prediction in the field. Sun used binary linear regression to build a model for predicting droplet deposition based on the operation height and the wind speed [15]. Yuan used the multivariate relevance vector machine (MRVM) regression method for building a nonlinear mapping model between the sprayer operating parameters and performance [16]. Regression analysis methods require less computation to build the prediction model than CFD. The datasets used by Sun [15] and Yuan [16] are from the CFD simulation results and are different from the real data in field experiments. In addition, the models only consider the relationship between droplet deposition and a few influencing factors. To build a more accurate prediction model, various factors related to droplet deposition must be considered comprehensively, requiring the algorithm for modeling to have a high learning ability. Deep learning has been widely used in agriculture because of its strong learning ability. Deep learning does not require professionals to define the characteristics of target data and has outstanding advantages in image processing and data analysis [17]. The common network types in deep learning include the convolutional neural network (CNN), recurrent neural network, deep belief network, and generative adversarial network (GAN), which have been used often in plant identification, disease detection, soil nutrient analysis, and yield prediction and achieved satisfactory results [18–20]. Studies that use deep learning are scarce in the field of aerial spraying. Wen used a GAN model to generate images of an UAV's flow-field distribution, and the similar images can also be generated by the CFD model [21]. The GAN model is superior to CFD models in terms of running speed and storage space. However, this model is unlikely to be adopted in actual agricultural production. The application of deep learning in aerial pest management is in its infancy and has not been verified in the field environment.

To solve the problems of traditional monitoring methods, such as the difficulty in deploying the large-scale sampling point of each field experiment, the time-consuming samples recovery, the complex detection process, and the high detection cost, a droplet deposition acquisition system (DDAS) needs to be developed based on a wireless sensor network. Environmental information can be collected by DDAS during UAV spraying, and then the droplet deposition can be calculated by the droplet deposition prediction model combined with the UAV spraying operation parameters. Given the superiority of deep learning, the prediction model in the DDAS will be programmed by a CNN algorithm. Since all the data used for model input in this study are one-dimensional data, a one-dimensional CNN (1D-CNN) structure was determined. Droplet deposition is influenced by many factors, and the 1D-CNN algorithm is suitable for solving such problems because of its excellent learning ability [22]. This study mainly consists of four parts:

(1) The data for building droplet deposition prediction model are collected through field experiments and then divided into different data sets according to the modeling requirements.
(2) The optimal structures of 1D-CNN models for predicting droplet deposition are established based on different data sets.
(3) The back propagation neural network (BPNN), the MRVM, and multiple linear regression (MLR) are used to build the models, and then these and the 1D-CNN model are compared.
(4) The droplet deposition prediction models are embedded in the DDAS, and the accuracy of the DDAS in terms of obtaining the droplet deposition is evaluated in comparison with WSP.

2. Materials and methods

2.1. *Development of DDAS*

To obtain the droplet deposition in real time and remotely, the DDAS is developed, which is composed of several sensor nodes. And each node consists of a temperature and

Please cite this article as: Z. Hao, M. Li, W. Yang et al., Evaluation of UAV spraying quality based on 1D-CNN model and wireless multi-sensors system, Information Processing in Agriculture, https://doi.org/10.1016/j.inpa.2022.07.004

humidity sensor, a wind speed sensor, a GPS sensor, a 4G data transmission module, and a processing unit. Raspberry Pi type 4B is used as the processing unit. The DDAS structure is shown in Fig. 1. The SHT35 temperature and humidity sensor (Sensirion, Switzerland) communicates with the Raspberry Pi through the I^2C communication protocol. The temperature measurement accuracy is ± 0.2 °C, and the humidity measurement accuracy is ± 1.5 % RH. Moreover, the temperature measurement range is from −40.0 °C to 125.0 °C, and the humidity measurement range is from 0.0 % RH to 100.0 % RH. The measurement error of the wind speed sensor (Openjumper, China) is ± 0.2 m/s, the measurement range is from 0.0 m/s to 55.6 m/s, and the output of the wind speed sensor is an analog signal. Given that Raspberry Pi does not have an analog-to-digital (A/D) conversion module, a PCF8591T module is used as the external A/D conversion module for Raspberry Pi to receive the voltage signal generated by the wind speed sensor. The PCF8591T module is an A/D conversion module based on I^2C with an 8-bit accuracy. To obtain the location information of the sampling site, a SIM7600CE 4G expansion board is added to Raspberry Pi. This expansion board is designed based on the Raspberry Pi 40 pin general-purpose input/output interface and is suitable for the Raspberry Pi motherboard. Moreover, the functions of the GPS, Beidou, and Glonass base station positioning methods and the 4G dial-up Internet access are supported by the SIM7600CE 4G expansion board with a global navigation satellite systems antenna interface and a SIM card. The latitude and longitude data of the sampling sites are obtained by the expansion board and transmitted to Raspberry Pi through a USB to UART interface based on the CP2102 oscillator. In addition, the Attention command is used by Raspberry Pi to obtain a 4G signal through the SIM7600CE 4G expansion board to realize the networking needs of the field. Then, the interaction between the DDAS hardware and the server database is realized through the 4G network. The data are obtained by the sensor nodes every 5 s and sent to the server. The DDAS uses the Ubuntu Server 18.04.1 LTS 64 built based on the Tencent Cloud Service with core cpu1, 2 GB RAM, and 2 Mbps network. The MySQL database is also configured in the server and is used as the data storage center of the DDAS. The writing part of the database is completed by Raspberry Pi, and the data reading and display are realized by the droplet deposition acquisition software on the Android smartphone. Under the Raspbian system, the MySQLdb library in Python language is used as the driver for Raspberry Pi to connect to MySQL. Under the premise that Raspberry Pi is connected to a 4G network, the environmental information obtained by the sensors is automatically written into the MySQL data table, which was built on Tencent Cloud server, and the operating parameters of UAV are manually written into the same data table. The droplet deposition acquisition software of the DDAS is installed on the smartphone Xiaomi10 pro (Android version: Android 10; SOC: Qualcomm Snapdragon 865). Under the premise of a smartphone connecting to the network, the MySQL connector Java package is used for data access to the cloud server database. The acquired data are processed by appropriate adapters to obtain the required data types. After the calculation based on the droplet deposition prediction model in the droplet deposition acquisition software, the software is combined with Baidu Map Android SDK for the visualization of the droplet deposition data on the smartphone.

2.2. *Experimental area and materials*

The experiments aimed to obtain a large amount of data for building the droplet deposition prediction model. The field experiments were designed to evaluate the objectives. The experiments were conducted in a commercial soybean field (36°15′35″ N and 116°37′11″ E) in Tai'an City, Shandong Province, China. The soybean type was Huanghuaihai summer soybean, and the variety was Zhonghuang 57. The plant spacing was 15 cm, and the row spacing was 45 cm. In the experiments, a XAG P20 plant protection UAV (Xaircraft, China) was used for the spraying operation (Fig. 2), and the key technical parameters of the UAV are shown in Table 1. The RTK

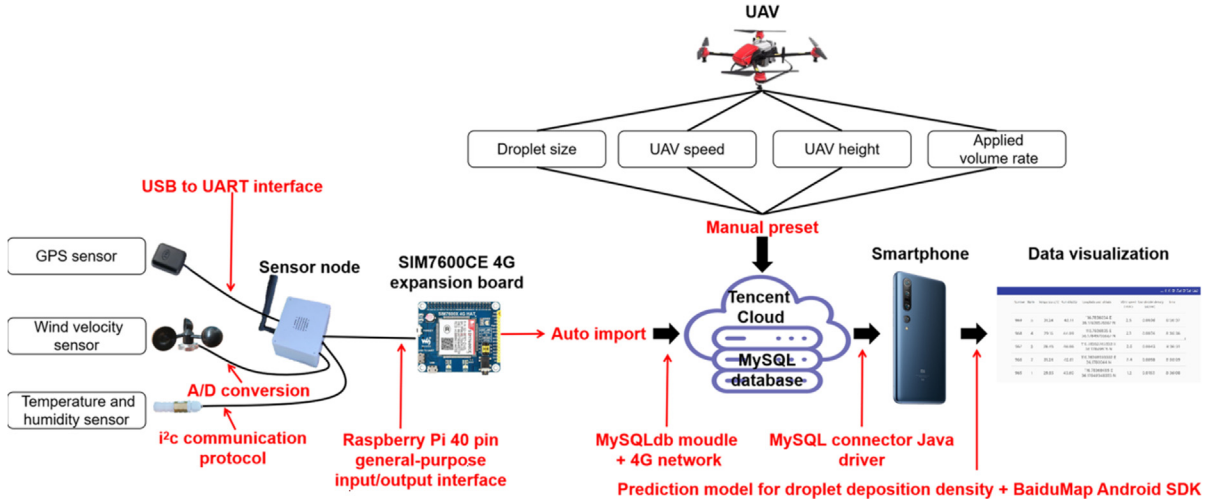

Fig. 1 – Structure of the developed DDAS (The black letter represents module of DDAS, and the red letter represents the method and technology of connecting the modules). (For interpretation of the references to colour in this figure legend, the reader is referred to the web version of this article.)

Please cite this article as: Z. Hao, M. Li, W. Yang et al., Evaluation of UAV spraying quality based on 1D-CNN model and wireless multi-sensors system, Information Processing in Agriculture, https://doi.org/10.1016/j.inpa.2022.07.004

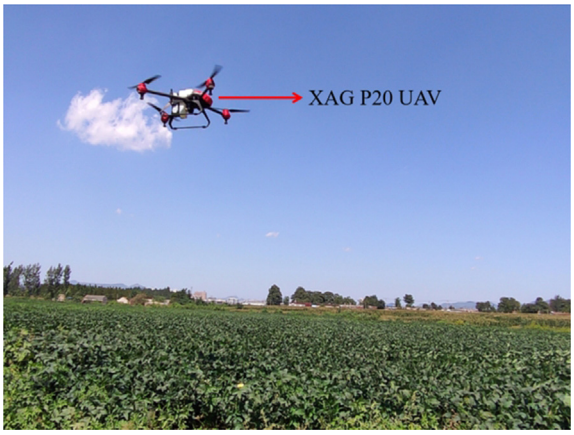

Fig. 2 – XAG P20 UAV used in field experiment.

(real-time kinematic) technology was used to achieve the positioning of UAV with centimeter-level accuracy. Moreover, the flight time of this UAV was 16 min without load and 8 min with fully loaded. In addition, the peristaltic pumps combined with the high-speed atomizing nozzles were used in the sprayer system of this UAV. The spraying flow rate was controlled by the peristaltic pumps and the atomization effect was controlled by the high-speed atomizing nozzles, which were controlled independently. The DDAS was used to record environmental information (initial temperature, initial humidity, the maximum humidity within 5 min after spraying, the minimum temperature within 5 min after spraying, and the average wind speed during the test), and a 3.1 cm × 8.1 cm WSP (Syngenta, Switzerland) was used to collect the deposited droplets.

2.3. *Experimental design*

In this study, soybeans with growth stages of 12, 23, 51, and 75 were selected for four experiments according to the Biologische Bundesanstalt, Bundessortenamt, and Chemical industry (BBCH)-scale [23], and the environmental conditions of each experiment are shown in Table 2. Because the experiments in each growth period took several days to complete, the experimental environmental parameters of the same growth period also had obvious differences. For the obtained droplets to be near the actual deposition state, WSP was clamped on the leaf of the soybean canopy at each sampling point, and the temperature and humidity sensor and wind speed sensor of the DDAS were also fixed near the WSP (Fig. 3). Given the need for many sample data to build an accurate model, the full factor experimental design was adopted. Through other relevant research [24] and the modifiable parameters of the XAG P20 plant protection UAV, four factors of the UAV spraying operation were selected, namely, droplet size, UAV spraying speed, UAV spraying height, and applied volume rate, to build the 1D-CNN. Meanwhile, these four parameters can be adjusted in the control terminal when the UAV performed spraying operations. The numerical level of each variable factor was defined according to the experimental environment and the key technical parameters of UAV. The combination design of factors and levels is shown in Table 3. On the basis of the full-factorial experimental design, 900 combinations were designed for testing in each experiment, and 900 sets of data were obtained. According to the experimental land characteristics, the flight route (Fig. 4) of UAV was determined. The flight parameters of the UAV spraying operations were changed three times in each flight, and three tests were carried out on flight paths 1, 2, and 3 of the flight routes. To reduce the error caused by the environment, five sampling points were set for each test to calculate the average value of the sampled data. In addition, all the sampling points were located directly below the flight path. A total of 3 600 sets of data (i.e., 900 sets of data in each experiment × 4 experiments) were obtained for modeling.

2.4. *Data collection*

After each experiment, the WSPs were collected and sealed immediately. After drying in the laboratory, the WSPs were scanned into digital images with a resolution of 600 dpi × 600 dpi using a high-resolution scanner (Epson, Japan), and the images were processed with the Deposit Scan software (Application Technology Research Unit, Wooster, OH, USA) to obtain the droplet deposition. In addition, the UAV spraying operation parameters (i.e., droplet size, UAV speed, UAV height, and applied volume rate) corresponding to the value of droplet deposition were recorded, and the environmental information recorded by the DDAS must also be saved. All these data were used for subsequent analysis and modeling.

2.5. *CNN model*

In this study, the deep learning algorithm was used to build the model for predicting the droplet deposition, and CNN

Table 1 – Key parameters of the UAV.

Items	Parameters
Rotor	Four rotors
Numbers of nozzles	4
Spraying width (m)	3
Peristaltic pump voltage (V)	32
Spraying flow rate (L/min)	0–5.6 (Adjust according to fixed grade)
Droplet size (μm)	85–550 (Adjust according to fixed grade)
Flight speed (m/s)	0–6 (Adjust according to fixed grade)
Operation height (m)	0–10 (Adjust according to fixed grade)
Maximum liquid load (kg)	10

Please cite this article as: Z. Hao, M. Li, W. Yang et al., Evaluation of UAV spraying quality based on 1D-CNN model and wireless multi-sensors system, Information Processing in Agriculture, https://doi.org/10.1016/j.inpa.2022.07.004

Table 2 – Main environmental parameters of the field experiments.

Experiment	Growth stage	Range of temperature(°C)	Range of humidity(%)	Range of wind velocity(m/s)
1	BBCH-12	17.2–25.8	30–76.3	0.9–3.3
2	BBCH-23	19–31.7	29–88.3	0.2–2
3	BBCH-51	23–34	51–90	1.1–3
4	BBCH-75	19.5–33.5	48–86.5	0.5–2.1

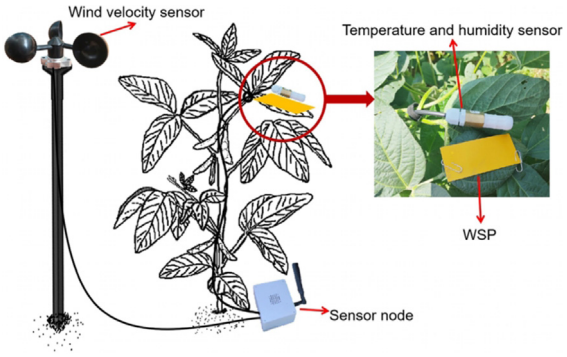

Fig. 3 – Deployment of WSP and DDAS for single soybean plant.

was used to extract the characteristics related to the droplet deposition mass. Feature extraction can be integrated with the multilayer perceptron by restructuring the CNN [25]. Therefore, CNN has a good adaptive performance and is also suitable for situations where the environmental information is complex and the inference rules are ambiguous. The input layer of the CNN model in this study is one-dimensional data, and the output after the regression analysis of the convolution and output layers is also one-dimensional data. Compared with two-dimensional CNN, 1D-CNN effectively uses the advantages of the convolution algorithm of less computational and hardware requirements and fast computational speed [26]. Therefore, the 1D-CNN structure was selected.

Convolution computation is an important part of the 1D-CNN, and the process is shown in Fig. 5. For a convolution layer of the 1D-CNN model, the inputs of the previous layer and the convolution kernels were convoluted to obtain the inputs of this layer, resulting in the following equation:

$$g_m^{l+1} = b_m^{l+1} + \sum_{n=1}^{N_l} f_{1D}(\omega_{nm}^l \times x_n^l), \quad (1)$$

where g_m^{l+1} is the mth input of the $l+1$th layer; x_n^l is the nth input of the lth layer; ω_{nm}^l is the convolution kernel weight between the nth input of the lth layer neuron and the mth input of the $l+1$th layer; b_m^{l+1} is the bias corresponding to the mth input of the $l+1$th layer; N_l is the total input number of the lth layer; f_{1D} represents a 1D-CNN convolution computation. In Eq. (1), the weights of the convolution kernels and the biases should be updated continuously, and the update process is shown in Fig. 6.

To show the ability of the 1D-CNN model in predicting droplet deposition, the common regression algorithms (i.e., BPNN, MRVM, and MLR) were used for comparison. BPNN is the most basic neural network with an excellent nonlinear mapping ability, which can be used for regression and classification problems [27]. By introducing the multinomial probability likelihood function, regression and multi-classification can be directly realized by the MRVM [16]. Meanwhile, MLR is a common regression modeling algorithm based on the least square method [28].

2.6. *Evaluation experiments of DDAS*

The experiment was carried out in the growth period of the BBCH-88 soybean to compare the consistency of the droplet deposition obtained by the DDAS and the WSP. The overall growth state of branches and leaves in the growth period of the BBCH-88 soybean was similar to that in the growth stages of 75. Five flights were designed in this experiment, and the route of each flight is the same, as shown in Fig. 4. In addition, 10 sampling points were located randomly under the flight route for each flight, which were different from the sampling point settings in Fig. 4. To prevent the distribution of sampled data from being too concentrated, some parameters were changed for each flight. In the evaluation experiments, the parameters that were changed were applied volume rate and UAV spraying height. The UAV parameter settings for each flight are shown in Table 4. During the experiment, the temperature, air humidity, and wind speed ranges were

Table 3 – Factors and levels in UAV spraying tests.

Factors	Levels					
	1	2	3	4	5	6
Droplet size(μm)	105	120	135	150	165	–
UAV spraying speed(m/s)	1	2	3	4	5	6
UAV spraying height(m)	2.5	3	3.5	4	4.5	–
Applied volume rate(L/ha)	6	9	12	15	18	21

Please cite this article as: Z. Hao, M. Li, W. Yang et al., Evaluation of UAV spraying quality based on 1D-CNN model and wireless multi-sensors system, Information Processing in Agriculture, https://doi.org/10.1016/j.inpa.2022.07.004

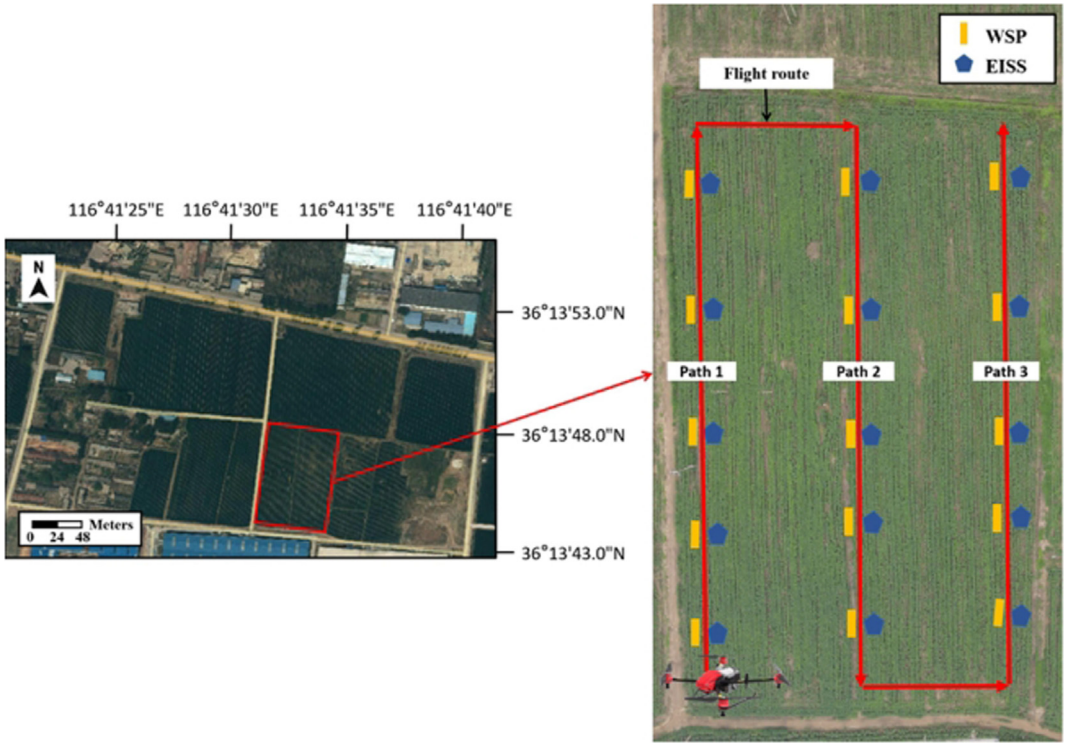

Fig. 4 – Schematic of sampling site and the route for each flight of UAV.

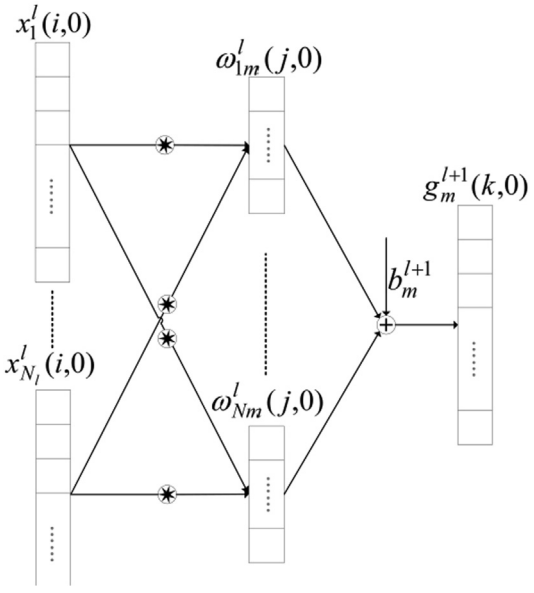

Fig. 5 – Schematic of one-dimensional convolution computation (Note: $0 \leqslant i \leqslant u-1$, $0 \leqslant j \leqslant v-1$, $0 \leqslant k \leqslant u-v$, where u is the length of each input, v is the length of each

22.9–32.1 °C, 38–72 %, and 2.2–3.0 m/s, respectively. The coefficient of determination (R^2, Eq. (2)) was used to evaluate the consistency of droplet deposition obtained by the two methods at 50 sampling points, and the root-mean-square error (RMSE, Eq. (3)) was used to evaluate the error of the DDAS.

$$R^2 = 1 - \frac{\sum_{i=1}^{m}(y_i - h(x_i))^2}{\sum_{i=1}^{m}(y_i - \frac{1}{m}\sum_{i=1}^{m}y_i)^2}, \quad (2)$$

$$RMSE = \sqrt{\frac{1}{m}\sum_{i=1}^{m}(h(x_i) - y_i)^2}, \quad (3)$$

where y_i is the true value of droplet deposition; $h(x_i)$ is the predictive value of droplet deposition; m is the total number of samples.

3. Results and discussion

3.1. 1D-CNN modeling

To analyze the relationship between different parameters and the droplet deposition and verify the accuracy of the model, two 1D-CNN models were built based on two data sets. (1) The droplet size, the UAV speed, the UAV height, the applied volume rate, and the average wind speed were used to form the basic data (BD); (2) Temperature and humidity data (the initial temperature, the initial humidity, the maximum humidity, and the minimum temperature) were combined with the BD to form the mixed data (MD). Both data sets were divided into three subsets: 3 200, 200, and 200 groups of data were used to form the training, validation, and test sets, respectively. The CNN model structure is based on the sequential model of the Keras deep learning framework, which consists of convolution, pooling, fully connected, and output layers. Keras is written in Python language, which can realize efficient optimization, parameter adjustment, and evaluation of deep networks. The training set was used

Please cite this article as: Z. Hao, M. Li, W. Yang et al., Evaluation of UAV spraying quality based on 1D-CNN model and wireless multi-sensors system, Information Processing in Agriculture, https://doi.org/10.1016/j.inpa.2022.07.004

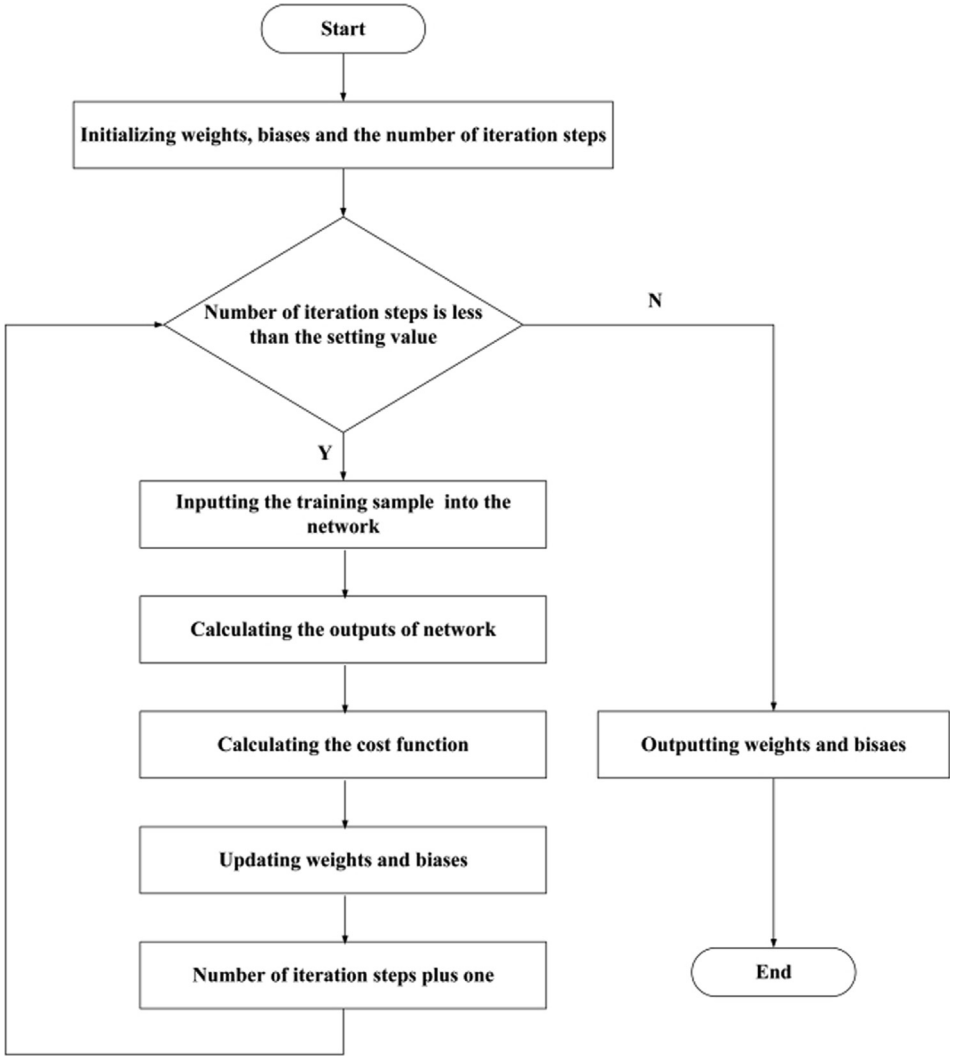

Fig. 6 – Update process of weights and biases.

Table 4 – UAV spraying operation parameters of each flight in the evaluation experiment.

Flight	Droplet size(μm)	UAV spraying speed(m/s)	UAV spraying height(m)	Applied volume rate(L/ha)
1	135	3	5	6
2	135	3	4	9
3	135	3	3	12
4	135	3	3	15
5	135	3	1	18

to build the 1D-CNN models, and the performance of the models was gradually adjusted by the validation set. Given few applications of 1D-CNN and no unified architecture, the model architecture in this study required exploration. In this study, the parameters of the two CNN models were empirically tuned multiple times. After tuning, the two structures with convergent results and high prediction accuracy were selected.

3.1.1. Determination of BD-based CNN model architecture

In previous studies, the relationship between various UAV parameters, wind speed, and other factors and the droplet deposition was often analyzed [29–31]. In this study, the BD was selected to establish the 1D-CNN model, and five parameters were used as input to the 1D-CNN model. After tuning the parameters in the 1D-CNN, the architecture of the designed BD-based CNN model was built as shown in Fig. 7,

Please cite this article as: Z. Hao, M. Li, W. Yang et al., Evaluation of UAV spraying quality based on 1D-CNN model and wireless multi-sensors system, Information Processing in Agriculture, https://doi.org/10.1016/j.inpa.2022.07.004

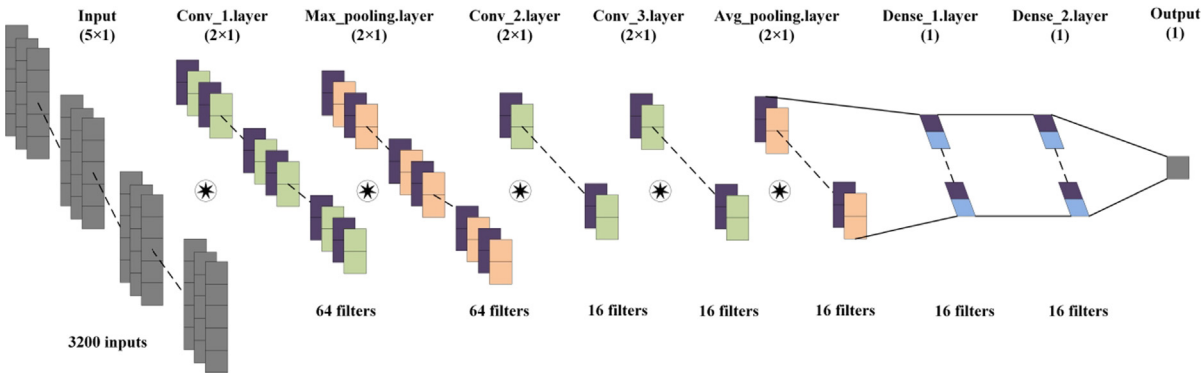

Fig. 7 – Architecture of the designed BD-based CNN.

consisting of 3 200 inputs (size: 5 × 1), three convolution layers, two pooling layers, two fully connected layers, and an output layer. The first convolution layer was defined as 64 filters with a convolution kernel size of 2 × 1. The output of the first neural network layer was a 4 × 64 matrix. The second layer added a maximum pooling layer with a convolution kernel size of 2 × 1 to reduce the complexity of the output and the over-fitting of the model, and the number of filters was 64. The second layer reduced the number of feature vectors output by the first convolution layer to half. Two additional convolution layers were added to learn the higher-level features, and the convolution kernel size of the two layers was 2 × 1, and the number of filters in the two layers was 16. Thus, the output after two convolution layers was a 1 × 16 matrix. The average pooling layer was added as the fifth layer to avoid over-fitting. In this layer, the convolution kernel size of filters was 2 × 1, and the number of filters was 16. The average value of the two weights was taken for pooling. The output matrix in this layer was 1 × 16, and only one weight was left after each filter passed through the fifth layer. Two fully connected layers were used to combine the features. The number of units of the fully connected layers was 16. After the sixth and seventh layers, the output was a 1 × 16 matrix. The final output layer obtained an output value, which was the output droplet deposition of the 1D-CNN model. The activation function of the output layer in the 1D-CNN was rectified linear unit (ReLU) because the regression problem was presented in this study, and the ReLU output was interval data. Similarly, the activation functions of the other hidden layers were also ReLU. The problem of gradient saturation could be solved by ReLU, which could accelerate the training speed of the model [32].

When the 1D-CNN was used to build a model, the input data required pre-processing, and normalization and standardization were performed to scale the data. Normalization transformed the data to [0, 1], and the data satisfied the standard normal distribution by standardization. If the order of magnitude of a sample input in a layer after the input layer is extremely large, then the output of this layer would enter the saturation interval in advance after the activation function. This condition causes the activation function to be insensitive to the feature. Therefore, the input of the 1D-CNN should be scaled, and batch normalization should be applied. Batch normalization standardized the statistical distribution of all samples. Meanwhile, each sample had its own statistical distribution, which could improve the generalization ability of the 1D-CNN.

The over-fitting of the 1D-CNN model should be considered due to the large numbers of neurons and network layers. The dropout was used to randomly set some weight values to 0, which could reduce the sensitivity of the network to small changes in data and avoid over-fitting. Five parameters of the dropout were tested, and the training loss of the 1D-CNN models is illustrated in Fig. 8. When the dropout was 0.5, 50 % of the neuron weights in the 1D-CNN model were randomly set to 0. In this situation, the training loss of the validation set did not increase much compared with the other values, and the sensitivity of the 1D-CNN model to small disturbances could also be reduced. The bigger dropout values would reduce the risk of over-fitting, therefore, 0.5 dropout was selected in the model.

The trends of training and validation losses with the number of iterations are shown in Fig. 9. The loss function of the training and validation set converged gradually with the

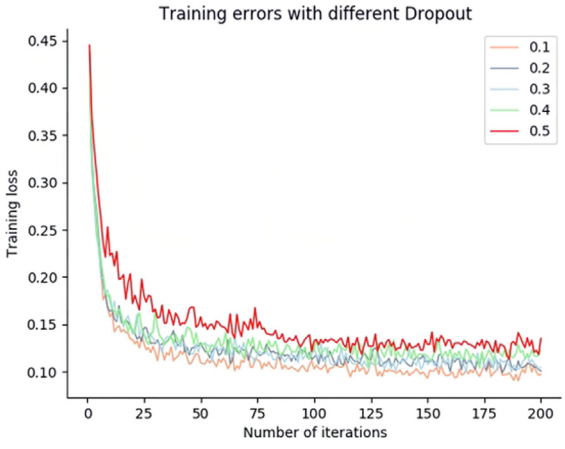

Fig. 8 – Training losses of BD-based CNN model with dropout parameters of 0.1, 0.2, 0.3, 0.4, and 0.5.

Please cite this article as: Z. Hao, M. Li, W. Yang et al., Evaluation of UAV spraying quality based on 1D-CNN model and wireless multi-sensors system, Information Processing in Agriculture, https://doi.org/10.1016/j.inpa.2022.07.004

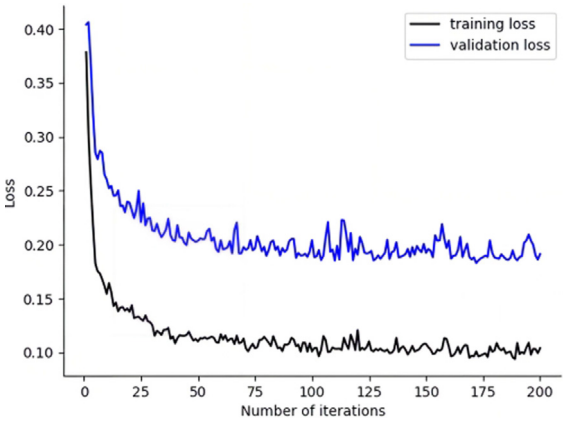

Fig. 9 – Training and validation losses of BD-based CNN model with the number of iterations.

increase in the number of iterations, indicating that the 1D-CNN prediction model could be used for the experimental dataset. After 125 training iterations, the value of training loss was stable at 0.1, and the value of validation loss was stable at 0.2. Meanwhile, the change rates of the loss function of the training and validation sets tended toward 0, indicating that the weights of the convolution layers completed the updating process.

3.1.2. *Determination of MD-based CNN model architecture*

Given the complexity of field environments, only using data, such as UAV parameters and wind speed, for modeling would result in the poor generalization ability of the model. During UAV spraying, the deposited droplets would not only be affected by the environment but also affect the environmental factors. After spraying, the water vapor concentration in the spraying area increased, the vapor pressure rose, and the relative humidity changed [33]. In addition, in the process of droplets deposition on the target crop, water evaporation reduced the radiation heat reaching the crop canopy, which led to the change in environmental temperature [34]. Therefore, the MD-based CNN model was established, which consisted of nine input parameters: the droplet size, the UAV spraying speed, the UAV spraying height, the applied volume rate, the average wind speed during the test, the temperature before spraying, the humidity before spraying, the maximum humidity within 5 min after spraying, and the minimum temperature within 5 min after spraying. The architecture of the MD-based CNN model consisted of 8 layers as shown in Fig. 10, including 3 200 inputs (size: 9 × 1), three convolution layers, two pooling layers, two fully connected layers, and an output layer. The first layer was a convolution layer with 64 filters, and the convolution kernel size of the filters was 3 × 1. The second layer was a maximum pooling layer, and the convolution kernel size was 3 × 1, and the number of filters was 64. The third layer was a convolution layer with 32 filters, and the convolution kernel size of the filters was 3 × 1. The fourth layer was a convolution layer with 16 filters, and the convolution kernel size of the filters was 3 × 1. An average pooling layer was added as the fifth layer, and the size of the convolution kernel was 3 × 1, and the number of filters was 16. The sixth and seventh layers were fully connected layers with 16 units. The eighth layer was the output layer, and the output was droplet deposition.

Similar to the BD-based CNN model, the activation functions of the output layer and other hidden layers in the MD-based CNN model were ReLU. Normalization, standardization, and batch normalization were also applied in the MD-based CNN model. In addition, the dropout was set to 0.5 (Fig. 11). The training process of the MD-based CNN model was completed after 150 training iterations (Fig. 12).

3.2. *Model evaluation*

3.2.1. *Modeling of different regression models*

BPNN, MRVM, and MLR were also used to build models based on the BD and the MD. For BPNN, three hidden layers were set, and the numbers of neurons were 128:36:1. Then, the BD- and MD-based BPNN models were built. For the MRVM, the kernel function was set as the radial basis function (RBF). Meanwhile, the penalty factor (C) of the error term was set to 1, and the coefficient (γ) of the RBF was set to 0.1. Thus, the BD- and MD-based MRVM models were built. The above hyper-parameters of BPNN and MRVM were the optimal choice after tuning. The BD- (Eq. (4)) and MD-based MLR (Eq. (5)) models were also built.

$$y_{BD} = 1.231x_{VR} + 0.037x_{DS} - 0.428x_{SH} - 0.2x_{SS} - 0.928x_{w} + 0.559, \quad (4)$$

and

$$y_{MD} = 0.967x_{VR} + 0.043x_{DS} - 0.094x_{SH} - 0.069x_{SS} + 0.405x_{H_0} + 1.378x_{H_{Max}} - 0.603x_{T_0} - 0.538x_{T_{Min}} - 0.158x_{w}, \quad (5)$$

where y_{BD} is the droplet deposition output of the BD-based MLR model; y_{MD} is the droplet deposition output of the MD-based MLR model; x_{VR} is the applied volume rate; x_{DS} is the droplet size; x_{SH} is the UAV spraying height; x_{SS} is the UAV spraying speed; x_{w} is the average wind speed; x_{H_0} is the humidity before spraying; $x_{H_{Max}}$ is the maximum humidity within 5 min after spraying; x_{T_0} is the temperature before spraying; $x_{T_{Min}}$ is the minimum temperature within 5 min after spraying.

3.2.2. *Models analysis*

The test set of BD was selected to evaluate the regression ability of the BD-based CNN, BPNN, MRVM, and MLR models, and the test set of MD was selected to evaluate the regression ability of the MD-based CNN, BPNN, MRVM, and MLR models. The R^2 and RMSE between the true and predicted values of the 8 models were calculated (Fig. 13). Some previous studies have shown that a small RMSE and a large R^2 correspond to the good prediction ability of the model [35–37]. The training and test sets had no duplicate data. Therefore, the validity of the test results could be guaranteed. The analysis results are shown in Fig. 13. The R^2 values of all the nonlinear models exceeded 0.7 (Fig. 13(a) to (f)). Meanwhile, the highest R^2 value of the MLR models was 0.632 (Fig. 13(h)), indicating a weak linear correlation between the inputs of the models and the droplet deposition and proving the necessity of using nonlinear

Please cite this article as: Z. Hao, M. Li, W. Yang et al., Evaluation of UAV spraying quality based on 1D-CNN model and wireless multi-sensors system, Information Processing in Agriculture, https://doi.org/10.1016/j.inpa.2022.07.004

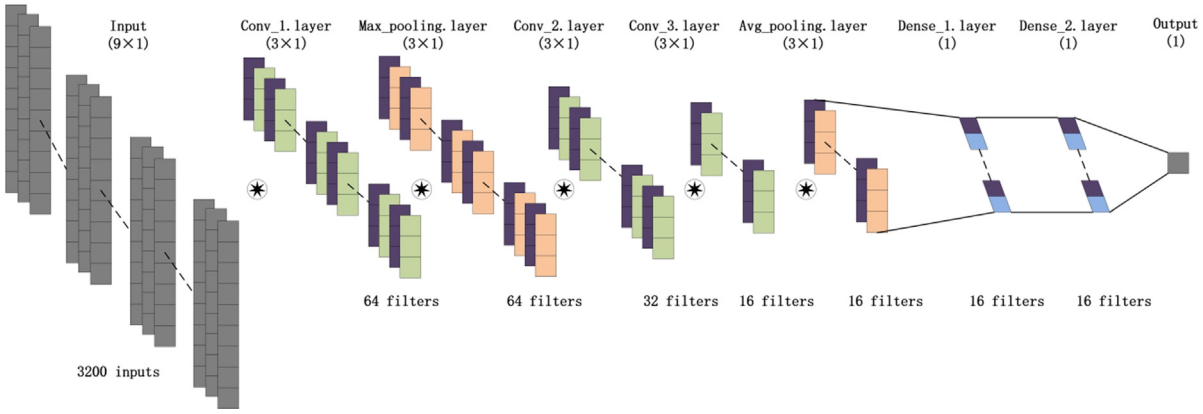

Fig. 10 – Architecture of the designed MD-based CNN.

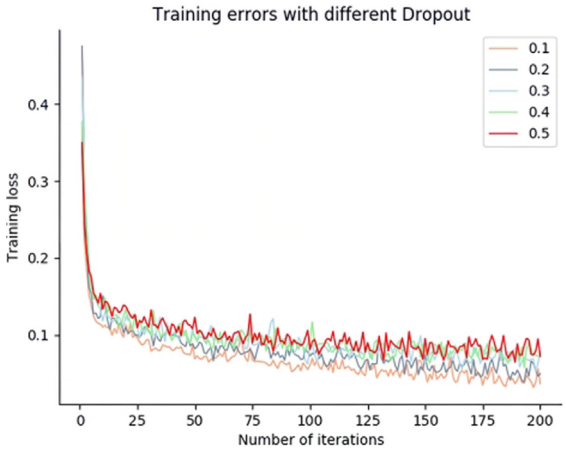

Fig. 11 – Training losses of MD-based CNN model with dropout parameters of 0.1, 0.2, 0.3, 0.4, and 0.5.

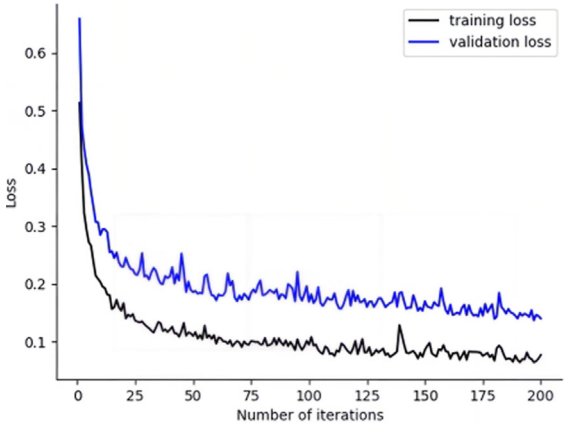

Fig. 12 – Training and validation losses of MD-based CNN model with the number of iterations.

models. Among the models compared, for the BD and the MD, the highest R^2 and lowest RMSE values were obtained by the CNN models (Fig. 13(b)). The R^2 and RMSE values of the MD-based CNN model were 0.981 and 0.066 μL/cm^2, and those of the BD-based CNN model were 0.86 and 0.181 μL/cm^2, respectively. For the same data set, the R^2 values of the BPNN models were lower than those of the 1D-CNN models, and the RMSE values were higher than those of the 1D-CNN models. Although BPNN and CNN have a similar training process, the convolution layers in the CNN architecture had better learning and analysis abilities on the experimental data than the fully connected layers in the BPNN architecture. Meanwhile, the risk of over fitting when the neural network needed to learn more parameters was avoided. Fig. 13(e) to (f) show that the R^2 values of both MRVM models exceeded 0.8, and the RMSE values were relatively low. Many data features were extracted through superposing the convolution layers of the 1D-CNN models, and more relationships among the parameters were analyzed to obtain the predicted results, which were near the true values. The 1D-CNN models exhibited better excellent ability to extract data features and a stronger generalization ability than the other traditional nonlinear regression models. The above analysis shows that among the three nonlinear regression algorithms shown in Fig. 13, the models established by the CNN algorithm exhibited the best prediction effect on droplet deposition.

The RMSE values of the eight models are shown in Fig. 13, indicating that the RMSE values of the MD-based models are lower than those of the BD-based models. The temperature and humidity data added to the input improved the prediction ability of the models for droplet deposition. Moreover, the MLR models could further prove the above conclusions. Obsie pointed out that the impact of each input of the MLR model on the output can be reflected by the coefficients of the model to a certain extent [38]. Eq. (4) reveals that the first three inputs, which contributed the most to the droplet deposition, were the applied volume rate, the average wind speed, and the UAV spraying height. Eq. (5) indicates that the first three inputs, which contributed the most to the droplet deposition, were the maximum humidity after spraying, the applied volume rate, and the temperature before spraying.

Please cite this article as: Z. Hao, M. Li, W. Yang et al., Evaluation of UAV spraying quality based on 1D-CNN model and wireless multi-sensors system, Information Processing in Agriculture, https://doi.org/10.1016/j.inpa.2022.07.004

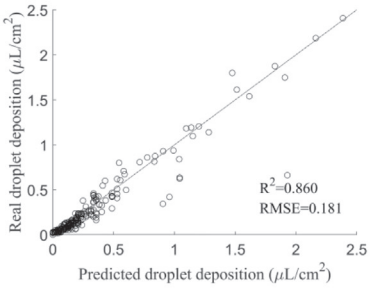

(a) BD-based CNN model

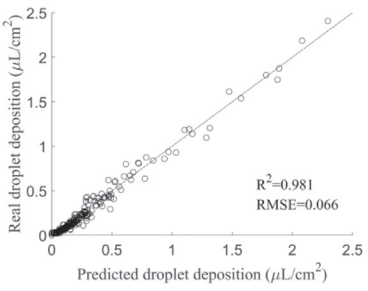

(b) MD-based CNN model

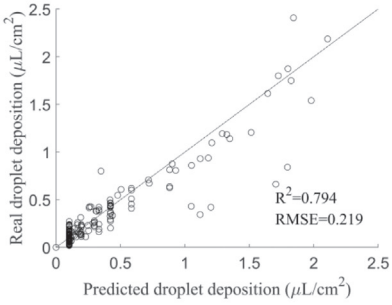

(c) BD-based BPNN model

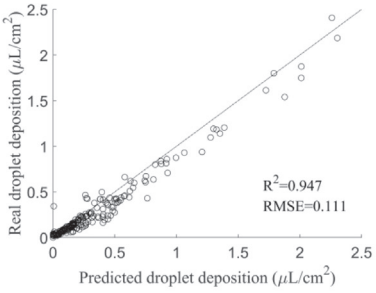

(d) MD-based BPNN model

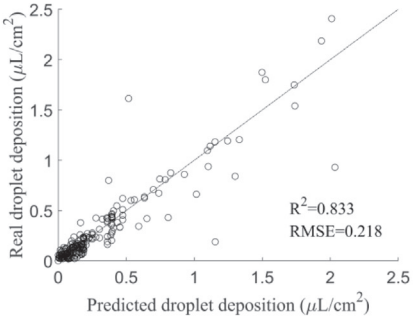

(e) BD-based MRVM model

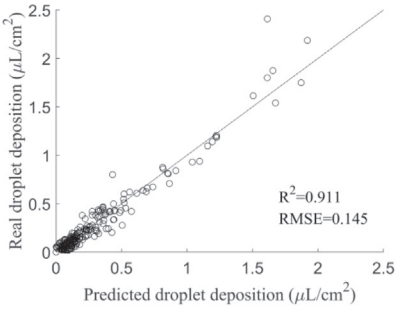

(f) MD-based MRVM model

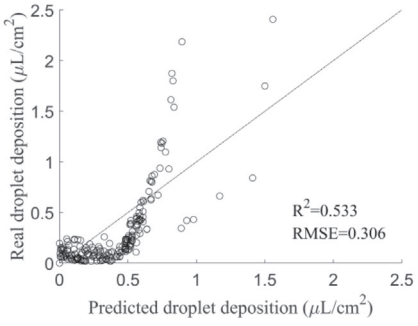

(g) BD-based MLR model

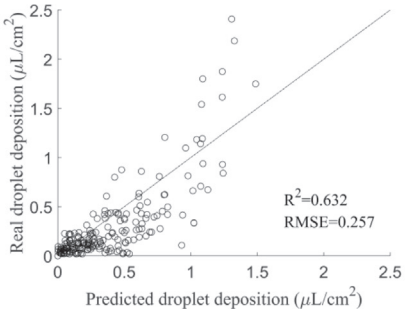

(h) MD-based MLR model

Fig. 13 – Scatter diagram of the comparison between predicted and real droplet depositions under eight models.

Please cite this article as: Z. Hao, M. Li, W. Yang et al., Evaluation of UAV spraying quality based on 1D-CNN model and wireless multi-sensors system, Information Processing in Agriculture, https://doi.org/10.1016/j.inpa.2022.07.004

The above analysis shows the necessity of adding environmental factors to the prediction of droplet deposition. In addition, the above analysis also shows that the applied volume rate and the UAV spraying height have greater impact on the droplet deposition than the other two UAV spraying operation parameters. Therefore, only the applied volume rate and the UAV spraying height were adjusted in the evaluation experiments of DDAS in the Section 2.6.

3.3. *DDAS evaluation*

To evaluate the application effect of the models in the DDAS, three models (i.e., the MD-based CNN, BPNN, and MRVM models) with R^2 values greater than 0.9 in Section 3.2 were selected for embedding in the DDAS. The accuracy of the DDAS in obtaining the droplet deposition was verified by the experimental method proposed in Section 2.6. The droplet deposition values obtained by the DDAS based on three models were compared with those obtained by WSPs (Fig. 14), and the results show that the R^2 and RMSE values of the DDAS based on the MD-based CNN model were 0.924 and 0.026 μL/cm^2, respectively, which had the highest accuracy in terms of obtaining the droplet deposition. During the DDAS evaluation experiment, due to the high wind speed in the environment, the droplet deposition values obtained by the DDAS were smaller than those of the test set in Section 3.2.2, and the range of droplet deposition was 0.021–0.302 μL/cm^2. Compared with the prediction results of the models on the test set data (Fig. 13(b), (d), (f)), the accuracy of predicting the droplet deposition decreased when the models were embedded in the DDAS for field experiments. The experimental site and crop were the same, but the crop growth state of the individual soybean was different, which might affect the accuracy of the models in the DDAS in predicting the droplet deposition. For this experiment, the biggest R^2 value still exceeded 0.9. Therefore, the DDAS based on the MD-based CNN model can be used for the real-time prediction of droplet deposition.

3.4. *Discussion*

At present, most of the research related t measuring droplet deposition selects a set of parameters corresponding to the best droplet deposition state from the limited spraying conditions, greatly limiting the guiding plant protection UAV

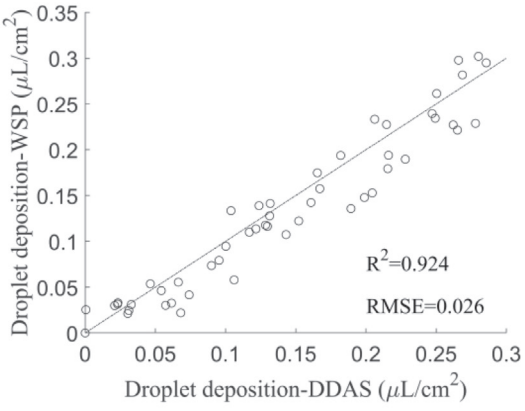

(a) DDAS with MD-based CNN model

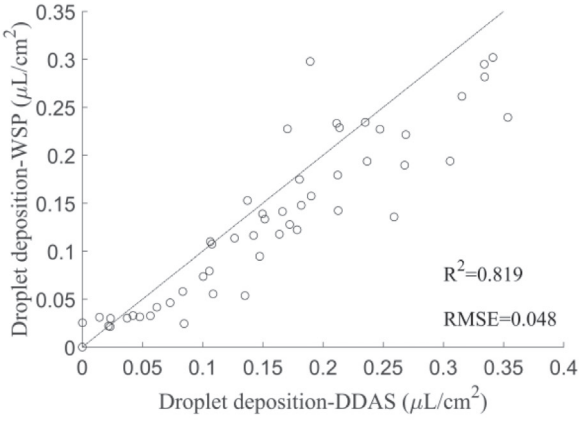

(b) DDAS with MD-based BPNN model

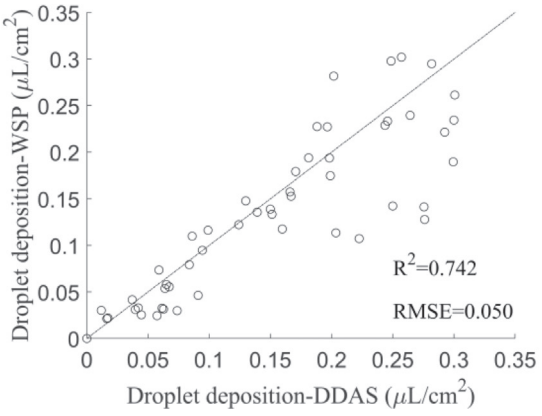

(c) DDAS with MD-based MRVM model

Fig. 14 – Scatter diagram of the comparison between droplet deposition - WSP and droplet deposition - DDAS.

Please cite this article as: Z. Hao, M. Li, W. Yang et al., Evaluation of UAV spraying quality based on 1D-CNN model and wireless multi-sensors system, Information Processing in Agriculture, https://doi.org/10.1016/j.inpa.2022.07.004

application in dynamic environments. The progress of research on the field application of plant protection UAV was analyzed [39], and results indicate that the research on the mechanism of the droplet deposition effect in the field of aviation plant protection is not intensive, and the correlation of factors affecting droplet deposition is weak. Therefore, the inference rule of the droplet deposition effect is unclear, and building a mathematical model with high accuracy is difficult. Hence, the idea of machine learning was introduced into the calculation of droplet deposition in this study, and the prediction models were established based on limited data to predict the droplet deposition under different spraying conditions to improve prediction accuracy. Related researches [22,40–42] show that the convolution layers of the 1D-CNN could extract and learn optimal features from the data, and the 1D-CNN model has advantages of accuracy and high speed compared with the traditional neural network. Therefore, the 1D-CNN algorithm was a suitable choice for building models for predicting droplet deposition. The effective features of the data related to droplet deposition could be extracted by the 1D-CNN algorithm, and the complicated mathematical analysis could be avoided during modeling. The results of the DDAS evaluation indicate that the 1D-CNN model established in this study indeed exhibits the best performance in terms of accuracy. The data in this study were all one-dimensional data, and the complexity of input data was low. Therefore, the 1D-CNN structures were not designed as complex deep structures. Meanwhile, to address the over fitting problem, only three convolution layers were designed, which could achieve the real-time prediction of droplet deposition. Abdoli pointed out that manual feature extraction was unnecessary for the original data when the modeling was based on the 1D-CNN. Moreover, fewer parameters were required by the 1D-CNN than the 2D-CNN, decreasing the amount of data for training [43]. Therefore, the 1D-CNN model is suitable for mobile devices or embedded systems. The above analysis indicates that the proposed 1D-CNN model has good practicability and could be embedded in the hardware system of the DDAS. The DDAS is still in the initial research stage and a new solution for remotely acquiring droplet deposition in real time. Wireless sensor network technology and a machine learning algorithm are integrated into the DDAS, which can make the DDAS arranged on a farm for a long time to realize the remote monitoring of droplet deposition, effectively addressing the shortcomings of labor-consuming and high-cost traditional droplet deposition detection methods. Therefore, the DDAS provides real-time data support for the evaluation of the spraying quality of plant protection UAV and has a high economic value. However, the DDAS must still be improved. The MD-based CNN model is the core of the DDAS for predicting droplet deposition, and the accuracy of predicting droplet deposition will be affected by the dimension of the data set. The DDAS evaluation results reveal that the prediction accuracy of the MD-based CNN model would decrease when the model is applied in different crop growth stages, which is related to the differences in crop canopy structures at different growth stages. The crop stems and leaves would be affected by the interaction between the UAV downwash airflow and the crops and show a cone-like vortex, which might affect the distribution of droplets on the canopy [39]. Therefore, attention should be given to the spraying droplet deposition of UAV in different growth stages of different crops. More droplet deposition data under different canopy structures must be collected to improve the 1D-CNN model in the future. In addition, the UAV parameters in the DDAS must be manually encoded at present. In subsequent studies, relevant sensors will be added to the UAV to realize the automatic acquisition of UAV parameters and improve the intelligence of the DDAS.

4. Conclusion

The proposed DDAS is composed of sensor nodes, the Tencent Cloud server with database, and the droplet deposition acquisition software based on Android. All field experimental data were obtained through UAV spraying experiments, and one measurement obtained two data sets, namely, the BD and the MD. The BD variables include the UAV spraying operation parameters and wind speed data, and the MD variables include the UAV spraying operation parameters, wind speed data, and temperature and humidity data. The 1D-CNN, BPNN, MRVM, and MLR models for the BD and the MD were established and analyzed. The main conclusions are as follows.

(1) The analysis of the prediction results of the BD- and MD-based CNN models, the BD- and MD-based BPNN models, the BD- and MD-based MRVM models, and the BD- and MD-based MLR models reveals that the RMSE values of the MD-based models were lower than those of the BD-based models built by using the same algorithms. Therefore, the prediction accuracy of the models was improved by adding temperature and humidity data, and these environmental factors cannot be ignored for modeling. In addition, the MD-based CNN model (1D-CNN) produced the best prediction result, namely, R^2 of 0.981 and RMSE of 0.066 μL/cm^2.
(2) MD-based CNN, BPNN, and MRVM models were embedded in the DDAS, and the accuracy of the DDAS in obtaining droplet deposition was verified through the comparison with WSPs in the field experiments. The results of the DDAS evaluation experiment show that the R^2 value of the droplet deposition obtained by the DDAS based on the MD-based CNN model and that by the WSPs was 0.924, and the RMSE was 0.026 μL/cm^2, which is the best among the three models.
(3) The remote acquisition of droplet deposition in real time can be realized by the DDAS with the MD-based CNN model, which can be extended to field applications and provide technical support for the intelligent evaluation of the quality of plant protection UAV spraying.

Declaration of Competing Interest

The authors declare that they have no known competing financial interests or personal relationships that could have appeared to influence the work reported in this paper.

Please cite this article as: Z. Hao, M. Li, W. Yang et al., Evaluation of UAV spraying quality based on 1D-CNN model and wireless multi-sensors system, Information Processing in Agriculture, https://doi.org/10.1016/j.inpa.2022.07.004

Acknowledgment

This study was supported by the National Key Research and Development Program of China (2019YFE0125500).

REFERENCES

[1] Otto A, Agatz N, Campbell J, Golden B, Pesch E. Optimization approaches for civil applications of unmanned aerial vehicles (UAVs) or aerial drones: a survey. Networks 2018;72(4):411–58. https://doi.org/10.1002/net.21818.

[2] Xue XY, Lan YB, Sun Z, Chang C, Hoffmann WC. Develop an unmanned aerial vehicle based automatic aerial spraying system. Comput Electron Agric 2016;128:58–66. https://doi.org/10.1016/j.compag.2016.07.022.

[3] Hilz E, Vermeer AWP. Spray drift review: The extent to which a formulation can contribute to spray drift reduction. Crop Prot 2013;44:75–83. https://doi.org/10.1016/j.cropro.2012.10.020.

[4] Chen SD, Lan YB, Li JY, Zhou ZY, Jin J, Liu AM. Effect of spray parameters of small unmanned helicopter on distribution regularity of droplet deposition in hybrid rice canopy in Chinese with English abstract. Trans Chin Soc Agric Eng 2016;32(017):40–6. https://doi.org/10.11975/j.issn.1002-6819.2016.17.006.

[5] Hoffmann WC, Hewitt AJ. Comparison of three imaging systems for water-sensitive papers. Appl Eng Agric 2005;21(6):961–4. https://doi.org/10.13031/2013.20026.

[6] Zhu HP, Salyani M, Fox RD. A portable scanning system for evaluation of spray deposit distribution. Comput Electron Agric 2011;76(1):38–43. https://doi.org/10.1016/j.compag.2011.01.003.

[7] Gao SC, Wang GB, Zhou YY, Wang M, Yang DB, Yuan HZ, et al. Water-soluble food dye of Allura Red as a tracer to determine the spray deposition of pesticide on target crops. Pest Manag Sci 2019;75(10):2592–7. https://doi.org/10.1002/ps.5430.

[8] Kirk IW. Measurement and prediction of atomization parameters from fixed-wing aircraft spray nozzles. Trans ASABE 2007;50(3):693–703. https://doi.org/10.13031/2013.23123.

[9] Acharya BS, Stebler E, Zou CB. Monitoring litter interception of rainfall using leaf wetness sensor under controlled and field conditions. Hydrol Processes 2017;31:240–9. https://doi.org/10.1002/hyp.11047.

[10] Lu J, Jia WD, Qiu BJ, Li PP. Experiment on retention of spray liquid on cucumber leaves in Chinese with English abstract. Trans Chin Soc Agric Mach 2010;41(4):60–4. https://doi.org/10.3969/j.issn.1000-1298.2010.04.013.

[11] Balsari P, Gil E, Marucco P, van de Zande JC, Nuyttens D, Herbst A, et al. Field-crop-sprayer potential drift measured using test bench: effects of boom height and nozzle type. Biosyst Eng 2017;154:3–13. https://doi.org/10.1016/j.biosystemseng.2016.10.015.

[12] Balsari P, Grella M, Marucco P, Matta F, Miranda-Fuentes A. Assessing the influence of air speed and liquid flow rate on the droplet size and homogeneity in pneumatic spraying. Pest Manag Sci 2019;75:366–79. https://doi.org/10.1002/ps.5120.

[13] Teske ME, Thistle HW, Mickle RE. Modeling finer droplet aerial spray drift and deposition. Appl Eng Agric 2000;16(4):351–7. Available from: https://doi.org/10.13031/2013.5216.

[14] Musiu EM, Qi LJ, Wu YL. Evaluation of droplets size distribution and velocity pattern using computational fluid dynamics modelling. Comput Electron Agric 2019;164. https://doi.org/10.1016/j.compag.2019.104886 104886.

[15] Sun GX, Wang XC, Ding WM, Zhang Y. Simulation analysis on characteristics of droplet deposition base on CFD discrete phase model in Chinese with English abstract. Trans Chin Soc Agric Eng 2012;28(6):13–9. https://doi.org/10.3969/j.issn.1002-6819.2012.06.003.

[16] Yuan J, Liu XM, Zhang XH, Zuo WL, Wang X, Chen LP. Modeling and compensation for characteristic of droplet drift on air-assisted boom spraying accounting for wind speeds. Trans Chin Soc Agric Eng 2013;29(014):45–52 [in Chinese with English abstract] https://doi.org/CNKI:SUN:NYGU.0.2013-14-007.

[17] Kamilaris A, Prenafeta-Boldu FX. Deep learning in agriculture: a survey. Comput Electron Agric 2018;147:70–90. https://doi.org/10.1016/j.compag.2018.02.016.

[18] Dyrmann M, Karstoft H, Midtiby HS. Plant species classification using deep convolutional neural network. Biosyst Eng 2016;151:72–80. https://doi.org/10.1016/j.biosystemseng.2016.08.024.

[19] Xu W, Wang QL, Chen RY. Spatio-temporal prediction of crop disease severity for agricultural emergency management based on recurrent neural networks. GeoInformatica 2018;22(4):363–81. https://doi.org/10.1007/s10707-017-0314-1.

[20] Guha P, Bhatnagar T, Pal I, Kamboj U, Mishra S. Prediction of properties of wheat dough using intelligent deep belief networks. J Exp Theor Artif In 2017;29:1283–96. https://doi.org/10.1080/0952813X.2017.1340976.

[21] Wen S, Shen NW, Zhang JT, Lan YB, Han J, Yin XC, et al. Single-rotor UAV flow field simulation using generative adversarial networks. Comput Electron Agric 2019;167. https://doi.org/10.1016/j.compag.2019.105004 105004.

[22] Ferreira LB, Cunha FFD. New approach to estimate daily reference evapotranspiration based on hourly temperature and relative humidity using machine learning and deep learning. Agric Water Manag 2020;234. https://doi.org/10.1016/j.agwat.2020.106113 106113.

[23] Munger P, Bleiholder H, Hack H, Hess M, Stauss R, Boom T, et al. Phenological growth stages of the soybean plant (glycine max l. merr.): codification and description according to the bbch scale. J Agron Crop Sci 1997;179(4):209–17. https://doi.org/10.1111/j.1439-037X.1997.tb00519.x.

[24] Qin WC, Qiu BJ, Xue XY, Chen C, Xu ZF, Zhou QQ. Droplet deposition and control effect of insecticides sprayed with an unmanned aerial vehicle against plant hoppers. Crop Prot 2016;85:79–88. https://doi.org/10.1016/j.cropro.2016.03.018.

[25] Abdeljaber O, Avci O, Kiranyaz MS, Boashash B, Sodano H, Inman DJ. 1-D CNNs for structural damage detection: verification on a structural health monitoring benchmark data. Neurocomputing 2017;275:1308–17. https://doi.org/10.1016/j.neucom.2017.09.069.

[26] Kiranyaz S, Ince T, Gabbouj M. Real-time patient-specific ECG classification by 1-D convolutional neural networks. IEEE T Bio-Med Eng 2015;63(3):664–75. https://doi.org/10.1109/TBME.2015.2468589.

[27] Shen H, Jiang Y, Li T, Cheng Q, Zeng C, Zhang L. Deep learning-based air temperature mapping by fusing remote sensing, station, simulation and socioeconomic data. Remote Sens Environ 2020;240:111692. https://doi.org/10.1016/j.rse.2020.111692.

[28] Li S, Yuan F, Ata-UI-Karim ST, Zheng H, Cheng T, Liu X, et al. Combining color indices and textures of UAV-based digital imagery for rice LAI estimation. Remote Sens 2019;11(15):1763. https://doi.org/10.3390/rs11151763.

[29] Musiu EM, Qi LJ, Wu YL. Spray deposition and distribution on the targets and losses to the ground as affected by application volume rate, airflow rate and target position. Crop Prot 2019;116:170–80. https://doi.org/10.1016/j.cropro.2018.10.019.

[30] Kharim MNA, Wayayok A, Shariff ARM, Abdullah AF, Husin EM. Droplet deposition density of organic liquid fertilizer at low altitude UAV aerial spraying in rice cultivation. Comput Electron Agric 2019;167. https://doi.org/10.1016/j.compag.2019.105045 105045.

[31] Ling W, Du C, Ze Y, xindong Ni, Shumao W. Research on the prediction model and its influencing factors of droplet deposition area in the wind tunnel environment based on UAV spraying. IFAC-PapersOnLine 2018;51(17):274–9. https://doi.org/10.1016/j.ifacol.2018.08.174.

[32] Ide H, Kurita T. Improvement of learning for CNN with ReLU activation by sparse regularization. In: 2017 International Joint Conference on Neural Networks. Anchorage, AK, USA; 2017. p. 2684–2691. https://doi.org/10.1109/IJCNN.2017.7966185.

[33] Chen LC, Bradley AA. Adequacy of using surface humidity to estimate atmospheric moisture availability for probable maximum precipitation. Water Resour Res 2006;42(9):350–9. https://doi.org/10.1029/2005WR004469.

[34] Liu HJ, Kang YH, Liu SP. Regulation of field environmental condition by sprinkler irrigation and its effect on water use efficiency of winter wheat in Chinese with English abstract. Trans Chin Soc Agric Eng 2003;19(6):46–51. https://doi.org/10.1049/el:20051702.

[35] Gao J, Chen R. An NEH-based heuristic algorithm for distributed permutation flowshop scheduling problems. Sci Res Essays 2011;6(14):3094–100. https://doi.org/10.5897/SRE10.1014.

[36] Li XL, He Y. Evaluation of least squares support vector machine regression and other multivariate calibrations in determination of internal attributes of tea beverages. Food Bioproc Tech 2010;3:651–61. https://doi.org/10.1007/s11947-008-0101-y.

[37] Lou SW, Li DHW, Lam JC, Chan WWH. Prediction of diffuse solar irradiance using machine learning and multivariable regression. Appl Energy 2016;181:367–74. https://doi.org/10.1049/10.1016/j.apenergy.2016.08.093.

[38] Obsie EY, Qu HC, Drummond F. Wild blueberry yield prediction using a combination of computer simulation and machine learning algorithms. Comput Electron Agric 2020;178. https://doi.org/10.1016/j.compag.2020.105778 105778.

[39] Li JY, Lan YB, Shi YY. Research progress on airflow characteristics and field pesticide application system of rotary-wing UAV. Trans Chin Soc Agric Eng 2018;34(12):104–18 [in Chinese with English abstract] https://doi.org/10.11975/j.issn.1002-6819.2018.12.013.

[40] Levent E, Turker I, Serkan KA. Generic Intelligent Bearing Fault Diagnosis System Using Compact Adaptive 1D CNN Classifier. J Signal Process Sys 2019;91:179–89. https://doi.org/10.1007/s11265-018-1378-3.

[41] Zhang M, Li W, Du Q. Diverse Region-Based CNN for Hyperspectral Image Classification. IEEE Trans Image Process 2018;27(6):2623–34. https://doi.org/10.1109/TIP.2018.2809606.

[42] Cao FL, Liu YH, Wang DH. Efficient saliency detection using convolutional neural networks with feature selection. Inf Sci 2018;456(1):34–49. https://doi.org/10.1016/j.ins.2018.05.006.

[43] Abdoli S, Cardinal P, Koerich AL. End-to-End Environmental Sound Classification using a 1D Convolutional Neural Network. Expert Syst Appl 2019;136:252–63. https://doi.org/10.1016/j.eswa.2019.06.040.

Please cite this article as: Z. Hao, M. Li, W. Yang et al., Evaluation of UAV spraying quality based on 1D-CNN model and wireless multi-sensors system, Information Processing in Agriculture, https://doi.org/10.1016/j.inpa.2022.07.004